JGR Oceans

RESEARCH ARTICLE
10.1029/2022JC018774

Sudden Reduction of Antarctic Sea Ice Despite Cooling After Nuclear War

Joshua Coupe[1,2,3], Cheryl Harrison[1,2], Alan Robock[3], Alice DuVivier[4], Elizabeth Maroon[5], Nicole S. Lovenduski[6], Scott Bachman[4], Laura Landrum[4], and Charles Bardeen[4]

[1]Department of Oceanography and Coastal Sciences, Louisiana State University, Baton Rouge, LA, USA, [2]Center for Computation and Technology, Louisiana State University, Baton Rouge, LA, USA, [3]Department of Environmental Sciences, Rutgers University, New Brunswick, NJ, USA, [4]National Center for Atmospheric Research, Boulder, CO, USA, [5]Department of Atmospheric and Oceanic Sciences, University of Wisconsin-Madison, Madison, WI, USA, [6]Department of Atmospheric and Oceanic Sciences, Institute of Arctic and Alpine Research, University of Colorado, Boulder, CO, USA

Key Points:

- A sudden reduction in Antarctic sea ice occurs despite global cooling after nuclear war in climate model simulations
- The sea ice changes in response to dynamic changes in atmospheric and oceanic circulation
- Even in a nuclear winter, Antarctic sea ice is vulnerable to wind shifts that cause upwelling of water onto the continental shelf

Supporting Information:

Supporting Information may be found in the online version of this article.

Correspondence to:

J. Coupe,
coupewx@gmail.com

Citation:

Coupe, J., Harrison, C., Robock, A., DuVivier, A., Maroon, E., Lovenduski, N. S., et al. (2023). Sudden reduction of Antarctic sea ice despite cooling after nuclear war. *Journal of Geophysical Research: Oceans*, *128*, e2022JC018774. https://doi.org/10.1029/2022JC018774

Received 27 APR 2022
Accepted 22 DEC 2022

Author Contributions:

Conceptualization: Joshua Coupe
Data curation: Charles Bardeen
Formal analysis: Joshua Coupe, Alice DuVivier
Funding acquisition: Alan Robock
Investigation: Joshua Coupe, Cheryl Harrison, Elizabeth Maroon, Nicole S. Lovenduski, Scott Bachman, Laura Landrum
Methodology: Joshua Coupe, Cheryl Harrison
Supervision: Cheryl Harrison, Alan Robock
Validation: Alice DuVivier
Visualization: Joshua Coupe
Writing – original draft: Joshua Coupe
Writing – review & editing: Joshua Coupe, Cheryl Harrison, Alan Robock, Alice DuVivier, Elizabeth Maroon, Nicole S. Lovenduski, Scott Bachman, Laura Landrum

Abstract A large-scale nuclear war could inject massive amounts of soot into the stratosphere, triggering rapid global climate change. In climate model simulations of nuclear war, global cooling contributes to an expansion of sea ice in the Northern Hemisphere. However, in the Southern Hemisphere (SH), an initial expansion of sea ice shifts suddenly to a 30% loss of sea ice volume over the course of a single melting season in the largest nuclear war simulation. In smaller nuclear war simulations an expansion in sea ice is instead observed which lasts for approximately 15 years. In contrast, in the largest nuclear war simulation, Antarctic sea ice remains below the long term control mean for 15 years, indicating a threshold that must be crossed to cause the response. Declining sea ice in the SH following a global cooling event has been previously attributed to shifts in the zonal winds around Antarctica, which can reduce the strength of the Weddell Gyre. In climate model simulations of nuclear war, the primary mechanisms responsible for Antarctic sea ice loss are: (a) enhanced atmospheric poleward heat transport through teleconnections with a strong nuclear war-driven El Niño, (b) increased upwelling of warm subsurface waters in the Weddell Sea due to changes in wind stress curl, and (c) decreased equatorward Ekman transport due to weakened Southern Ocean westerlies. The prospect of sudden Antarctic sea ice loss after an episode of global cooling may have implications for solar geoengineering and further motivates this study of the underlying mechanisms of change.

Plain Language Summary Firestorms from a global nuclear war would generate large amounts of smoke that could enter the Earth's atmosphere and block sunlight. Climate model simulations that inject smoke into the upper atmosphere confirm that this smoke causes rapid global cooling leading to increased sea ice in the Northern Hemisphere. However, sea ice in the Southern Hemisphere actually shrinks in the 2–6 years after a very large nuclear war, mainly caused by a change in the winds around Antarctica. Smoke heats the upper atmosphere and the westerly winds around Antarctica shift closer to the coast. The wind shift causes Ekman transport of the top layer of the ocean away from the coast, which brings up relatively warm water from below, melting sea ice during summer and inhibiting sea ice growth during the winter. A similar response has been found in simulations of supervolcano eruptions. As greenhouse gasses continue to warm up the Earth's oceans, a global cooling event that triggers a similar wind shift may lead to greater reductions in Antarctic sea ice.

1. Introduction

Ice in the Southern Ocean is sensitive to various types of climate change. Anthropogenic global warming threatens ice shelves that hang off the Antarctic coastlines, along with the marine communities that inhabit them, via ice sheet thinning and, in extreme cases, ice shelf collapse (Mayewski et al., 2009). Global-warming-induced climate change, working in tandem with the now recovering ozone hole, has contributed to a positive trend in the Southern Annular Mode (SAM) (e.g., Fyfe et al., 2007), which leads to a poleward shift in the mid-latitude westerly winds (Spence et al., 2014). A poleward shift in the westerlies tends to weaken the polar easterly winds, which help to maintain the Antarctic Slope Front, a dynamical oceanic barrier preventing significant heat exchange on the Antarctic continental shelf with relatively warm circumpolar deep water (Spence et al., 2014). The strength and positioning of this front in response to changes in the winds can be highly consequential for Antarctic sea ice, as intrusions of circumpolar deep water onto the continental shelf cause substantial basal melting (Dinniman et al., 2012). Weakened polar easterlies also decrease the amount of downward Ekman

pumping along the Antarctic coastlines, increasing the chance that relatively warm subsurface water can be transported upward onto the continental shelf and melt sea ice (Meehl et al., 2019). As the background sea surface temperature (SST) increases, Antarctic sea ice faces increased vulnerability (Meehl et al., 2019). The stability of Antarctic sea ice has been discussed extensively in the context of anthropogenic climate change (e.g., Dinniman et al., 2012; Fyfe et al., 2007; Mayewski et al., 2009; Meehl et al., 2019; Reese et al., 2018; Spence et al., 2014), but fewer studies have examined the impact of a sudden global cooling event, natural or otherwise, on Antarctic sea ice (e.g., McCusker et al., 2015; Verona et al., 2019; Zanchettin et al., 2014).

Volcanic eruptions are natural events known to cause global cooling by injecting sulfuric gases into the upper atmosphere, which become sulfate aerosols that can block solar radiation from reaching the surface (Robock, 2000). Both modern and historical volcanic eruptions have been linked to warming near the Antarctic Peninsula in response to changes in wind stress in a manner resembling the positive phase of the SAM (Verona et al., 2019). Differential heating of volcanic sulfate aerosols in the Southern Hemisphere (SH) upper troposphere and lower stratosphere can strengthen the stratospheric polar vortex, causing a poleward shift of the westerlies and producing a positive SAM. The same mechanism that threatens to upwell warm subsurface water onto the continental shelf if global warming continues unabated also appears to be responsible for environmental changes after volcanic eruptions. In simulations of supervolcano eruptions, an initial increase in Antarctic sea ice after an eruption is followed by a sharp drop 24–36 months later, suggesting a threshold where global cooling events can trigger sudden sea ice loss (Zanchettin et al., 2014). A geoengineering modeling study found that sulfate aerosol injections into the stratosphere designed to slow global warming could not preserve the West Antarctic Ice Sheet because changes to the atmospheric circulation increased water temperatures around ice shelves, increasing basal melting (McCusker et al., 2015). Warming oceans due to anthropogenic greenhouse gas emissions only increase the potential for a sudden global cooling event to cause sudden reductions in Antarctic sea ice in the future. Understanding a threshold where atmospheric circulation changes can initiate Antarctic sea ice loss is crucial because as the base temperature state of the oceans increases, this threshold could change.

Nuclear war driven firestorms are one of the more extreme potential stratospheric aerosol injection events with drastic consequences for global climate, with some scenarios potentially surpassing some of the most impactful volcanic eruptions in recorded history (Table S1 in Supporting Information S1). In recent years, large-scale wildfires with exceptionally large pyrocumulonimbus clouds have injected up to 0.9 Tg of soot into the stratosphere, altering stratospheric chemistry but having limited impacts to the surface climate (Yu et al., 2021). Unlike wildfires, in a large-scale nuclear war, massive firestorms across many different urban centers with higher fuel loading densities could produce up to 150 Tg of smoke with a greater percentage of black carbon, which absorbs more solar radiation and "self-lofts" the smoke into the stratosphere and higher.

Here, we perform the first analysis of impacts of a nuclear winter on Antarctic sea ice through climate modeling experiments. Nuclear war's environmental impact has been explored previously using climate models to investigate other aspects of the climate system (Coupe et al., 2019, 2021; Harrison et al., 2022). As up to 150 Tg of smoke enters the upper atmosphere, sudden climate change is likely as solar radiation is blocked from reaching the ground (Coupe et al., 2019; Robock et al., 2007). Freezing temperatures in the mid-latitudes during summer time can be observed in Earth system model simulations of large-scale nuclear war between the United States and Russia, which could severely impact global agriculture (Coupe et al., 2019; Xia et al., 2022) and fisheries (Scherrer et al., 2020). The Northern Hemisphere (NH) winter time circulation and the El Niño-Southern Oscillation (ENSO) become highly perturbed for many years as black carbon heats the stratosphere and cools the equatorial oceans (Coupe & Robock, 2021; Coupe et al., 2021). Cooling at high latitudes triggers both a short term and decadal scale expansion of Arctic sea ice (Harrison et al., 2022). However, in these same simulations, there is an initial expansion of Antarctic sea ice, followed by a sudden reduction 2–3 years after the onset of nuclear winter and then a slower return to pre-nuclear winter ice concentration. We investigate the mechanisms behind these sea ice changes to understand what drives a near collapse of Antarctic sea ice in a nuclear winter and provide insight about possible responses to smaller global cooling events.

2. Data and Methods

To model the impact of a nuclear war on the climate, we use the Community Earth System Model (CESM, version 1.3) with the Whole Atmosphere Community Climate Model Version 4 (WACCM4) as the atmospheric component. The atmospheric component has a horizontal resolution of 1.9° × 2.5° with 66 vertical layers and

a 140 km model top (Marsh et al., 2013). The ocean model component is the Parallel Ocean Program (POP, version 2) which has a nominal horizontal resolution of 1°, 60 vertical levels (Danabasoglu et al., 2012). The ice model component is version 4 of the Los Alamos Sea Ice Model, Community Ice CodE (CICE4) (Hunke & Lipscomb, 2008), which takes into account the deposition of aerosols like black carbon onto the ice surface. The CO_2 concentration in all simulations is 367 ppm, equivalent to that measured in the year 2000. To simulate a nuclear war, soot (black carbon) is injected into the upper troposphere and lower stratosphere in a layer between 100 hPa and 300 hPa over a one week period starting on 15 May of what will be referred to as "Year 0." Soot is evenly distributed horizontally over the countries involved in each nuclear war scenario. We use the Community Aerosol and Radiation Model for Atmospheres (CARMA), a sectional aerosol model coupled to WACCM4, which treats black carbon aerosols as fractal particles (Bardeen et al., 2017). CARMA has 21 different size bins for the aerosols with different optical properties, allowing particle growth to change the amount of absorption and scattering. Hygroscopic growth is not included, but particles coagulate together at a rate which is partially a function of relative humidity. This provides a realistic simulation of soot growth, transport, and deposition.

In total, six nuclear war scenarios are examined. Five India and Pakistan nuclear war scenarios are considered which involve soot injections of 5, 16, 27.3, 37, and 46.8 Tg. These simulations are each run for 15 years and three simulations of the 5 Tg case were conducted to separate internal climate variability. A United States and Russia scenario is represented with a 150 Tg soot injection, which is run for 30 years. We focus on the 150 Tg United States and Russia case and a 46.8 Tg India and Pakistan case, hereafter referred to as NW-150 Tg and NW-46.8 Tg, respectively. India and Pakistan cases were developed by Toon et al. (2019), while the 150 Tg United States and Russia scenario is a legacy case that assumes both countries use most of their nuclear arsenals on each other's cities (Robock et al., 2007), which is still possible with today's nuclear arsenals. 150 Tg of soot emissions into the upper atmosphere is assumed to be produced by 3,100–4,400 nuclear warheads with yields between 100 and 500 kilotons targeted at military and industrial areas in the United States and Russia. The NW-46.8 Tg simulation assumes 500 nuclear weapons with an average yield of 100 kilotons are detonated on military and urban targets in India and Pakistan. In the smallest 5 Tg case, 44 weapons with an average yield of 15 kilotons are used. Soot is injected into the upper atmosphere by the ensuing firestorms in cities within the target areas that would last for days. General climate changes from these simulations have been reported previously by Coupe et al. (2019) and Toon et al. (2019). Three ensemble members of a 20-year unperturbed control run are conducted to compare with the perturbed cases. In all simulations, the ocean model is initialized from a previously spun-up simulation using year 2000 radiative forcing. A long term spin-up of the ocean physical state was not possible due to limited computer resources, but small drifts in deep ocean temperature have caused no meaningful trends in sea ice extent, volume, or surface temperature in the control run.

The model configuration used here is similar to what is used in an assessment of CESM with WACCM4 and CICE4 by Marsh et al. (2013), who found that while the model overestimates Antarctic sea ice extent during the SH minimum in February and March, there is agreement with observations during the SH maximum between August and November. While CESM-WACCM4-CICE4 does not perfectly match the observed retreat of sea ice between the maximum and minimum, it performs better than the previous iteration of CESM, the Community Climate System Model. The sudden changes to Antarctic sea ice in the simulations performed for this study contrast the weakened seasonal cycle during normal model conditions, indicating a limited role for this bias to influence the primary results discussed here. This version of the model does not have interactive freshwater flux from melting ice shelves and instead uses a prescribed flux from the land model. Beyond the sea ice model itself, WACCM simulations of SH circulation, atmospheric temperature, and ozone are within the error estimates of historical trends (Marsh et al., 2013). At the same time, in response to both depleted polar stratospheric ozone and increased greenhouse gas concentrations, the model simulates a poleward shift in the SH polar vortex, which tends to reduce sea ice extent (Smith et al., 2012). Periods with a poleward shifted jet produce reduced sea ice extent in this model configuration, consistent with prior work. Variations in Antarctic sea ice extent and volume in our model's control run are not statistically different from those in the CESM Large Ensemble (Kay et al., 2015; Singh et al., 2021; Figure 1), despite using a different atmospheric model. The model's moderate successes bolster our confidence in this model configuration's ability to reasonably simulate sea ice changes during a nuclear winter, an event which thankfully cannot be validated and hopefully never will.

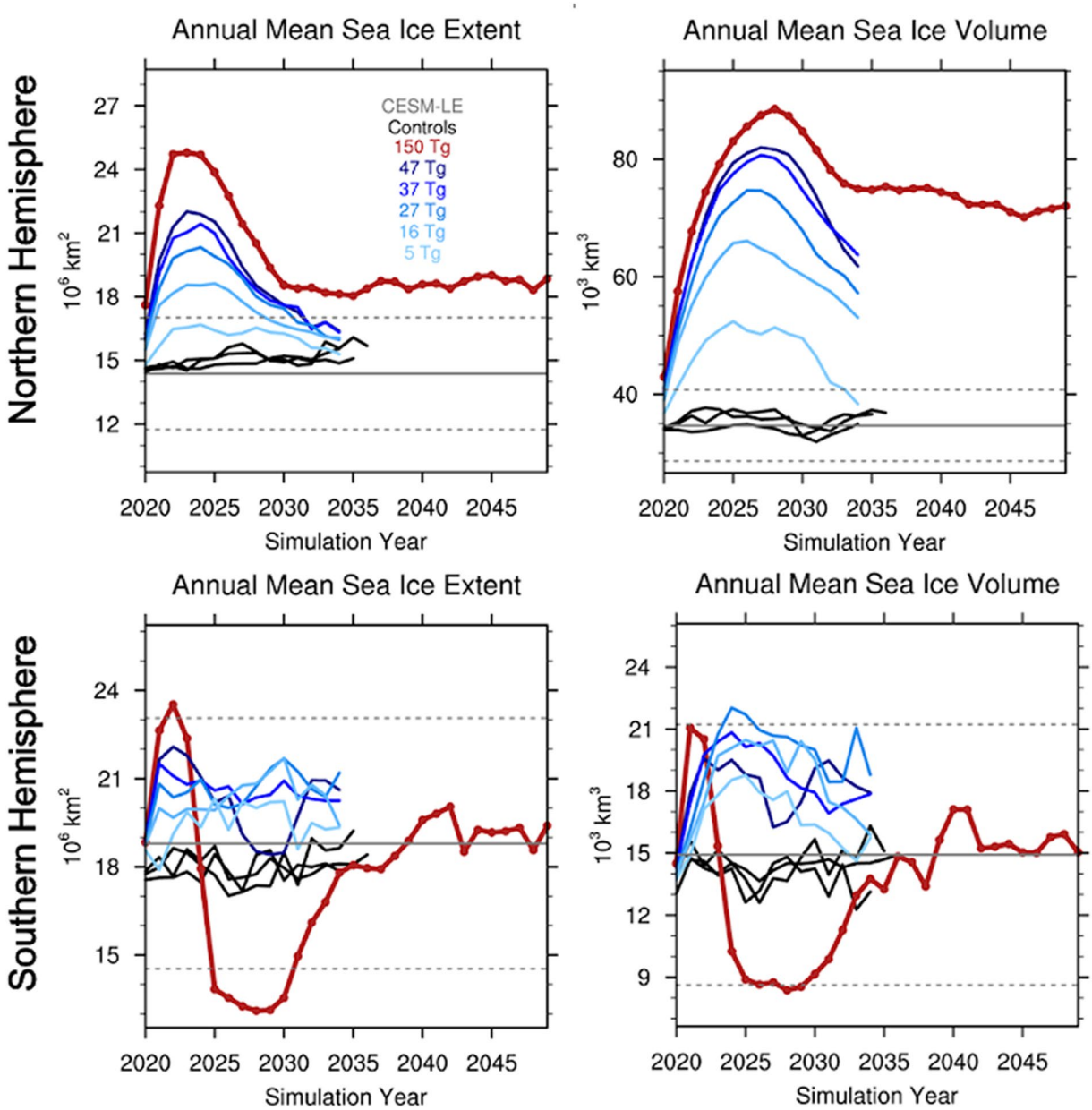

Figure 1. Annual mean sea ice extent (left) and volume (right) in the Northern Hemisphere (top) and Southern Hemisphere (bottom) in six simulations of nuclear war, a control run, and a CESM-LE pre-industrial simulation. The injection of soot is on 15 May in Year 0. The solid line indicates the CESM-LE pre-industrial mean and the dashes are ±1 standard deviation from the mean.

3. Results

3.1. Sea Ice Changes After Nuclear War

Within months of a nuclear war between the United States and Russia, as simulated in NW-150 Tg, soot aerosols block sunlight over the Arctic, allowing for an anomalous expansion of sea ice (Figure 1). Global mean surface temperatures decline by nearly 10°C in 3 years in NW-150 Tg while surface solar radiation anomalies exceed −100 W m^{-2} (Figure S1 in Supporting Information S1). A robust NH polar vortex and poleward shifted tropospheric jet help to keep colder air over the northern pole, strengthening the tropospheric polar high which favors enhanced sea ice growth in the Arctic. Across nuclear war scenario simulations where at least 16 Tg of soot is injected into the upper atmosphere, a significant increase in NH sea ice area and volume is simulated (Figure 1). Sea ice extent remains well above the control mean for up to 30 years after the initial soot injection in NW-150 Tg,

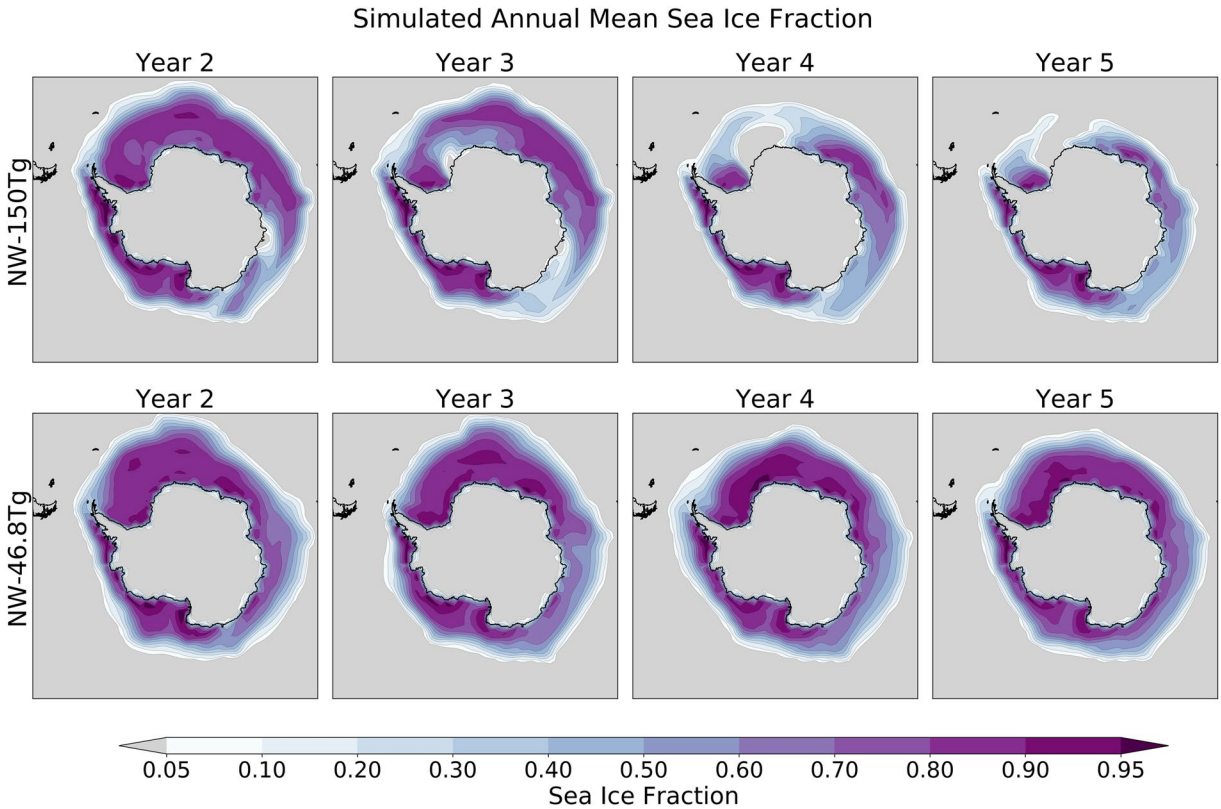

Figure 2. Annual mean sea ice fraction for NW-150 Tg (top) and NW-46.8 Tg (bottom) from years 2 to 5. The injection of soot is on 15 May in Year 0. An initial expansion of sea ice occurs in both simulations, followed by a sudden decline in NW-150 Tg between years 2 and 3.

suggesting a new, expanded equilibrium state of NH sea ice after this largest nuclear war scenario. During this 30 year period, global mean surface temperatures also remain 0.5°C below the control mean in NW-150 Tg, likely driven by sea ice albedo feedbacks and lagging deep ocean temperatures.

Unexpectedly, there is an asymmetric sea ice response between the hemispheres in NW-150 Tg, which has also been observed in simulations of supervolcanic eruptions, such as Toba and Yellowstone (Zanchettin et al., 2014). In the SH, an expansion of sea ice area and volume initially occurs within the first 2 years of a nuclear war due to reduced solar radiation and cooling associated with that loss of energy. Even for a higher latitude soot injection, sunlight is blocked in the SH within 6 months because global coverage of soot is achieved due to the high buoyancy of the smoke and the winds of the stratosphere. All sectors of Antarctic sea ice initially expand under global cooling due to the global soot layer. When soot aerosol forcing is increased to 150 Tg, the trend of increasing sea ice sharply reverses between years 3 and 4 of the simulation, when a sudden reduction of sea ice occurs (Figure 1), driven by changes in the Weddell Sea. This change is present in NW-150 Tg and not in NW-46.8 Tg.

A polynya, which is an area of open water surrounded by ice, develops in the Weddell Sea in NW-150 Tg (Figure 2), originating from the coast approximately 2 years and 5 months post-injection, eventually spreading outwards until the polynya reaches open ocean during the boreal summer in year 3–4 of NW-150 Tg. A gap in sea ice extends from Antarctica to the open ocean in the Weddell Sea throughout the entire winter (JJA) of year 5, before sea ice begins to build back in year 6. By year 6, solar radiation received at the surface is approaching 90% of normal conditions (Figure S1 in Supporting Information S1) because most of the soot aerosols have been removed by this time, reducing their influence on atmospheric circulation. In the western Weddell Sea, just east of the Antarctic Peninsula, both NW-150 Tg and NW-46.8 Tg exhibit anomalously low sea ice extent (Figure 3) along with surface warming (Figure 4). These features are reminiscent of the response that has been well documented after volcanic eruptions like the June 1991 Mt. Pinatubo eruption, and have been linked with a weakening of the Weddell Gyre (Verona et al., 2019). We investigate the mechanisms behind the sudden reduction in sea ice in Section 3.2 and find they are closely linked to changes in surface winds around Antarctica.

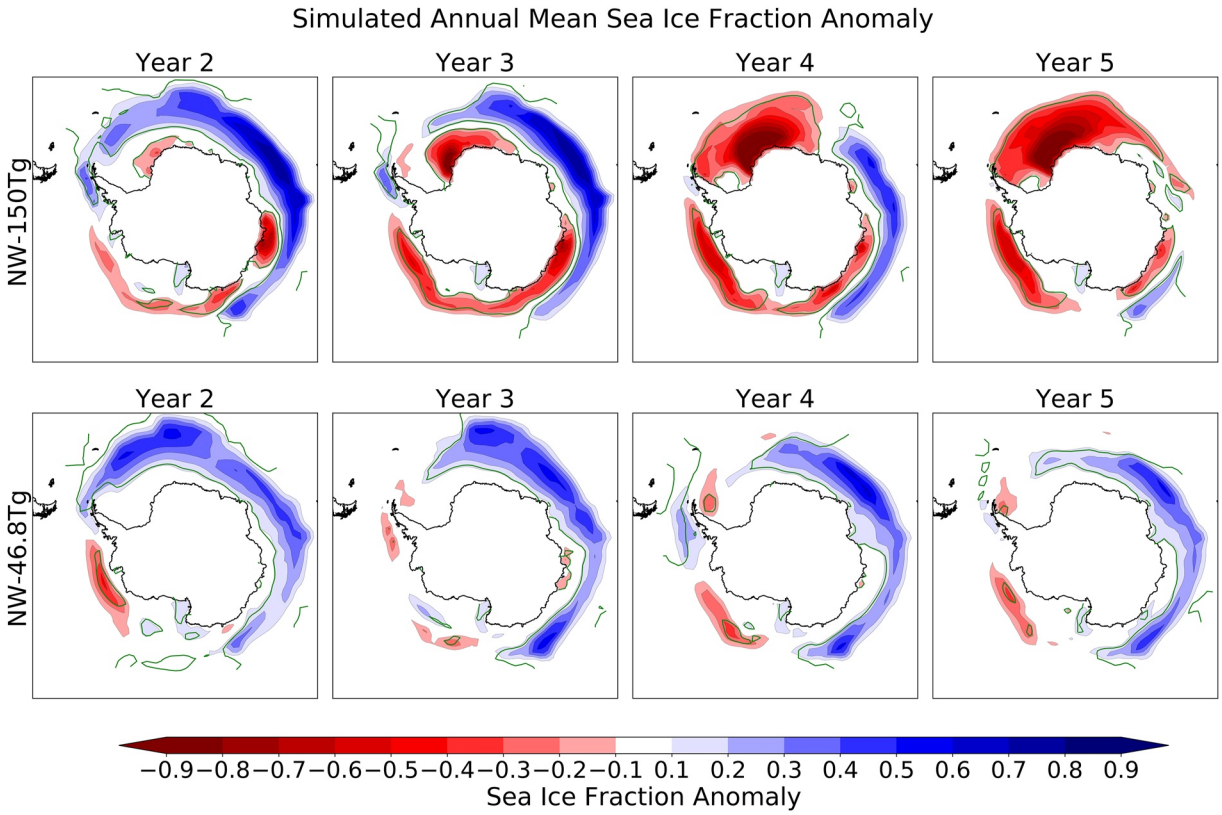

Figure 3. Annual mean sea ice fraction anomaly for NW-150 Tg (top) and NW-46.8 Tg (bottom) between years 2 and 5. The injection of soot is on 15 May in Year 0. Anomalies are calculated with respect to 60 years of a control run mean. Green contour indicates areas where the anomalies are statistically significant beyond ±2 standard deviations.

Across other sectors there is also substantial sea ice loss at the same time that the Weddell Sea polynya develops (Figure 3). In the Pacific sector, sea ice loss occurs on the edge of the continent, a feature present in both NW-150 Tg and NW-46.8 Tg, and the amount of loss scales with the initial injection amount. In the Indian Ocean sector there is sea ice loss along the coast in NW-150 Tg, while only minimal changes are simulated in NW-46.8 Tg. Together, these results show that sea ice can be suddenly lost in the Weddell Sea and other regions when additional soot is injected into the upper atmosphere. In all sectors with sea ice losses, the sudden reduction is closely associated with sudden surface warming (Figure 4), an important factor in the non-linearity of the Weddell Sea response. To investigate the mechanisms for sea ice loss further, we examine each sector.

3.2. Mechanisms for Antarctic Sea Ice Loss

3.2.1. Nuclear Niño and the Pacific Sector

Global climate change in the aftermath of a nuclear war includes anomalously warm SST in the eastern equatorial Pacific that persist for 6–7 years. This response has been described as a "Nuclear Niño," characterized by an incredibly strong and long-lasting excitement of the positive phase of ENSO in response to a massive injection of soot aerosols into the stratosphere (Coupe et al., 2021). Increasing SST contributes to an unusual amount of convective activity and rising air in the eastern Pacific, which helps to generate an anomalous Rossby wave train that perturbs the atmospheric circulation pattern, causing large variations in Antarctic sea ice extent and volume. Specifically, the strength of the Amundsen Sea Low (ASL) tends to be weaker during the positive phase of ENSO (Paolo et al., 2018; Raphael et al., 2016). On the other hand, enhanced convective activity in the eastern Indian Ocean and western Pacific Ocean during a period of La Niña has also been linked to a sharp reduction in Antarctic sea ice from September to November of 2016 (Meehl et al., 2019). During this episode in late 2016, a Rossby wave train emanating from enhanced convective activity in the eastern Indian Ocean set up an anomalously strong low in the Amundsen Sea that extended toward the Weddell Sea, favoring a significant retreat of Antarctic sea ice across multiple sectors. The ASL exerts substantial influence on the sea ice off Western Antarctica by

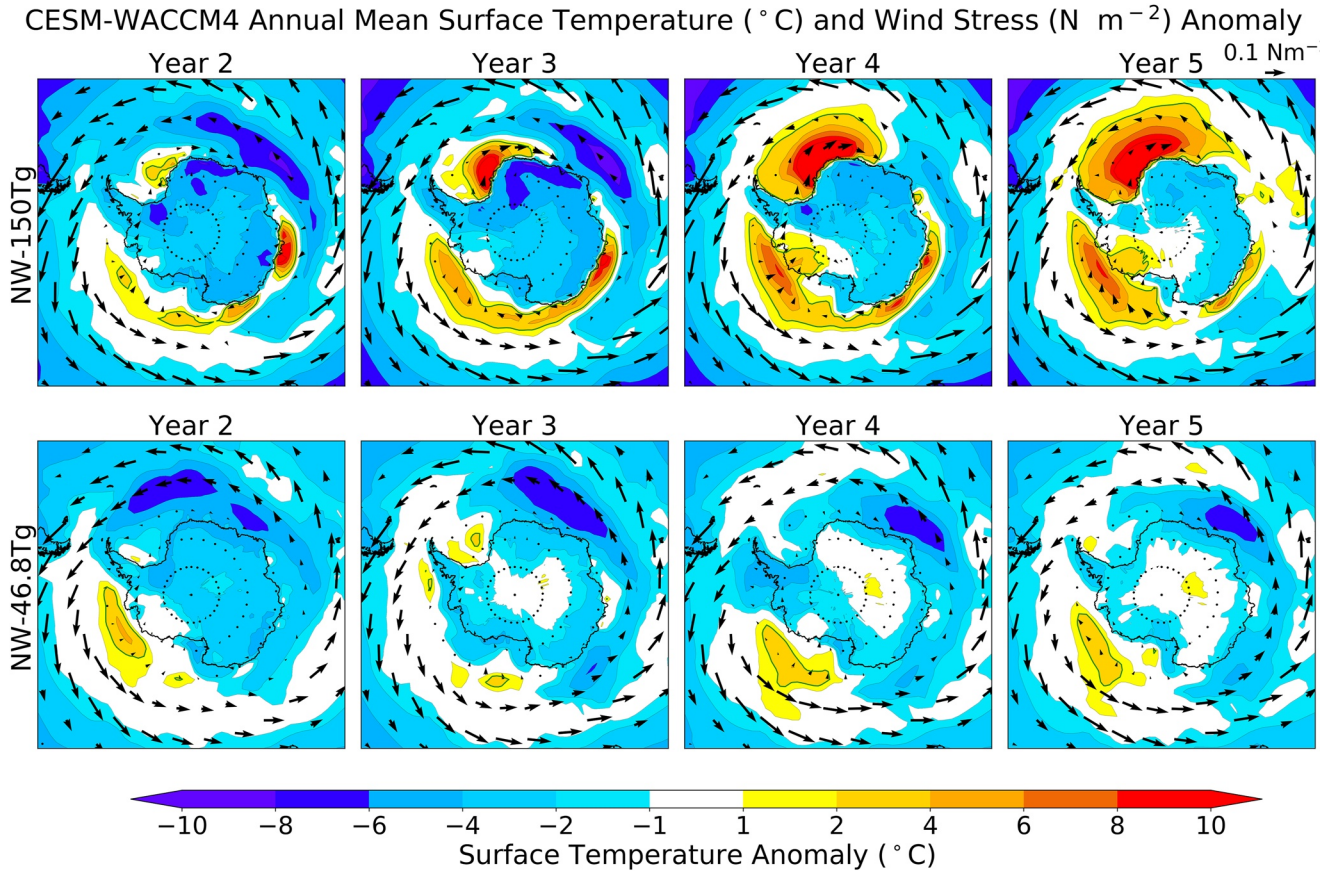

Figure 4. Annual mean surface temperature anomaly for NW-150 Tg (top) and NW-46.8 Tg (bottom) between years 2 and 5. The injection of soot is on 15 May in Year 0. Zonal and meridional wind stress anomalies are shown as black vectors (N m^{-2}) and indicate anomalously easterly surface winds across the Southern Ocean, assisting in driving the thermodynamic anomalies. Green contour indicates areas where the anomalies are statistically significant beyond +2 standard deviations.

affecting distributions of temperature and snowfall. After a nuclear war, there is a significant weakening of the ASL, connected to ENSO's reorganization of the atmospheric circulation. Mean sea level pressure is anomalously high across all of Antarctica in NW-150 Tg, influencing the pressure gradient in the Southern Ocean which can impact the winds.

To quantify the potential impact of ENSO on Antarctic sea ice in our simulations, we constructed a composite of surface temperature, sea ice fraction, and wind stress anomalies for all "El Niño months" by averaging together all months in the control run ensembles where the Niño3.4 SST anomaly is greater than 1.0°C. This is illustrated in Figure 5a, which shows that in the control run climatology, El Niño is associated with higher surface temperatures and negative sea ice fraction anomalies along Western Antarctica north of the Amundsen and Ross Seas. Weakened westerlies in the Southern Ocean and subtly poleward meridional wind stress anomalies in the Amundsen Sea contribute to the warming signal. ENSO-related circulation anomalies are associated with dipole patterns of sea ice changes, with sea ice loss in the Pacific sector and sea ice growth in the Weddell Sea and Indian Ocean. These patterns are similar to those seen in observations (e.g., Stammerjohn et al., 2008). Although changes to the mean climate state from global cooling may affect teleconnections between ENSO and Antarctic sea ice, the same teleconnection patterns can be identified in simulations of nuclear war. This mechanism is dependent on an accurate model depiction of ENSO, its teleconnections with the mid-latitude and high latitude circulation pattern, and those pattern's effects on sea ice.

ENSO is linked to wind stress changes around Antarctica by its influence on the strength and positioning of the ASL, as well as the amplitude of the Southern Annular Mode (SAM; Ding et al., 2012; Lachlan-Cope & Connolley, 2006). The SAM is quantified as the first EOF of 700 hPa geopotential heights from 20° to 90°S, a methodology also used by the Climate Prediction Center (CPC, 2021). A composite of months with a SAM index below −2.0 is shown in Figure 5b. There are strong similarities between an El Niño and a negative SAM

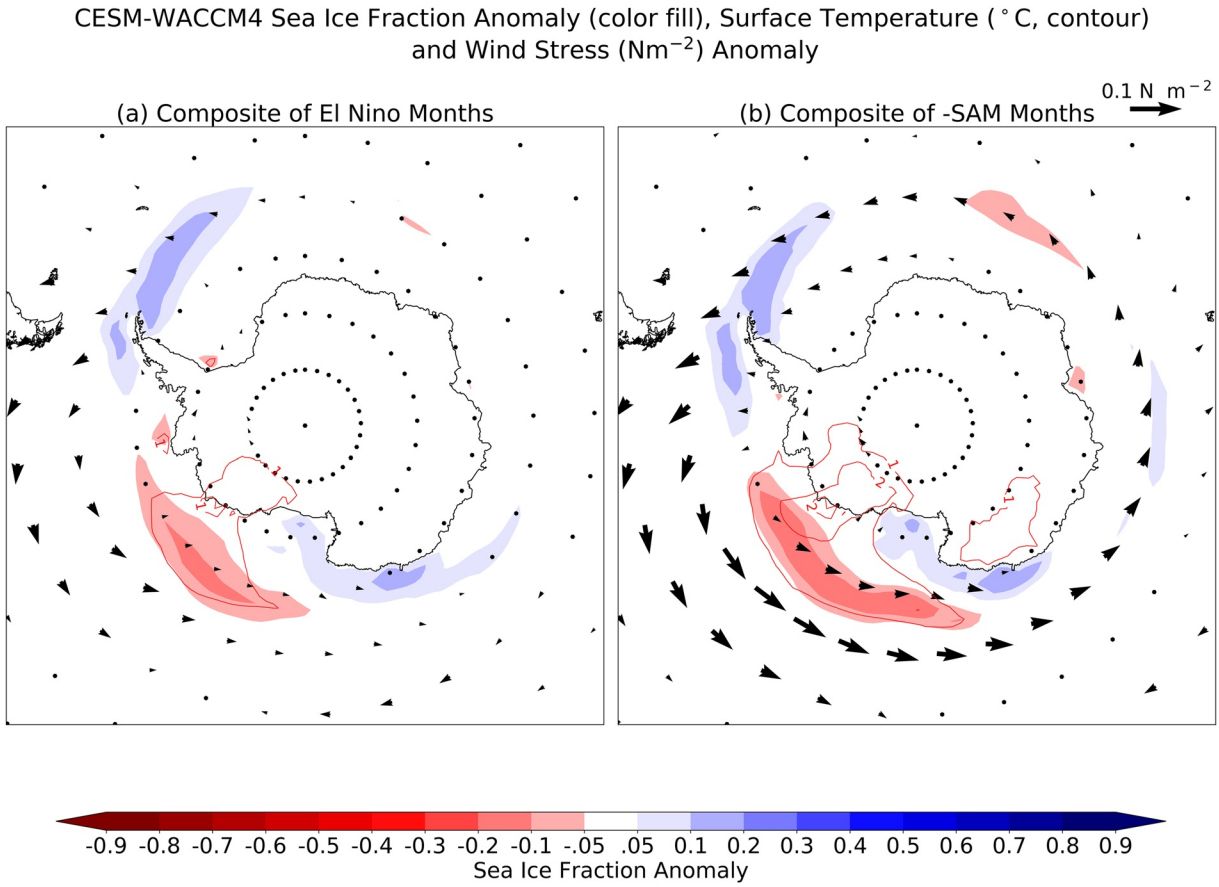

Figure 5. CESM-WACCM4 control run composite of (a) El Niño conditions and (b) negative Southern Annular Mode (SAM) conditions (less than −1.0) on Antarctic sea ice extent anomalies (color fill), surface temperature anomalies (red contour), and surface wind stress anomalies (N m^{-2}, vectors). Similarities between conditions during El Niño and negative SAM indicate significant overlap between these modes of climate variability.

in CESM-WACCM4 because the weakening of the ASL in response to El Niño dominates the first EOF of geopotential heights and surface pressure. This produces a negative SAM pattern, despite a strengthened polar jet in the stratosphere and upper troposphere. After a nuclear war, the ASL is weakened and the polar jet is shifted poleward, leading to weakened Southern Ocean westerlies and increased advection of relatively warm air over sea ice just offshore of West Antarctica. This halts sea ice development during the winter and accelerates sea ice melt during austral summer when El Niño peaks. Therefore, a small increase in atmospheric meridional heat transport from ENSO-related changes to atmospheric circulation contributes to Antarctic sea ice loss in the Pacific sector (encompassing the Amundsen-Bellingshausen and Ross Seas). These circulation anomalies endure during the period when El Niño dominates, contributing to the continuous decline in annual mean sea ice extent for 6–7 years. However, ENSO-related circulation anomalies do not explain sea ice loss in the Weddell Sea or Indian Ocean, indicating there are competing mechanisms.

3.2.2. Ekman Suction Contributes to Warming in the Weddell Sea

The Weddell Sea experiences the most rapid sea ice loss in the 2–5 years following a 150 Tg stratospheric soot injection, aided by the formation of a polynya that begins near the Antarctic coast and spreads out to the northern edge of the Weddell Sea (see Figure 2). Naturally occurring Weddell Sea polynya formation is rare but has occurred during the austral winters of 1974–1976 (Kurtakoti et al., 2018) and during the anomalous Antarctic sea ice retreat event in austral spring of 2016 (Meehl et al., 2019; Turner et al., 2017). Weddell Sea polynyas can be simulated using a relatively low resolution model (Cheon et al., 2015; Hirabara et al., 2012), enabling simulation here of polynyas following a nuclear war. Modeling studies have found three conditions that can precondition the Weddell Sea region for sustained convection and polynya formation, including (a) sufficient heat content of Weddell Deep Water, (b) strong negative wind stress curl over the Weddell Sea, and (c) anomalously high surface

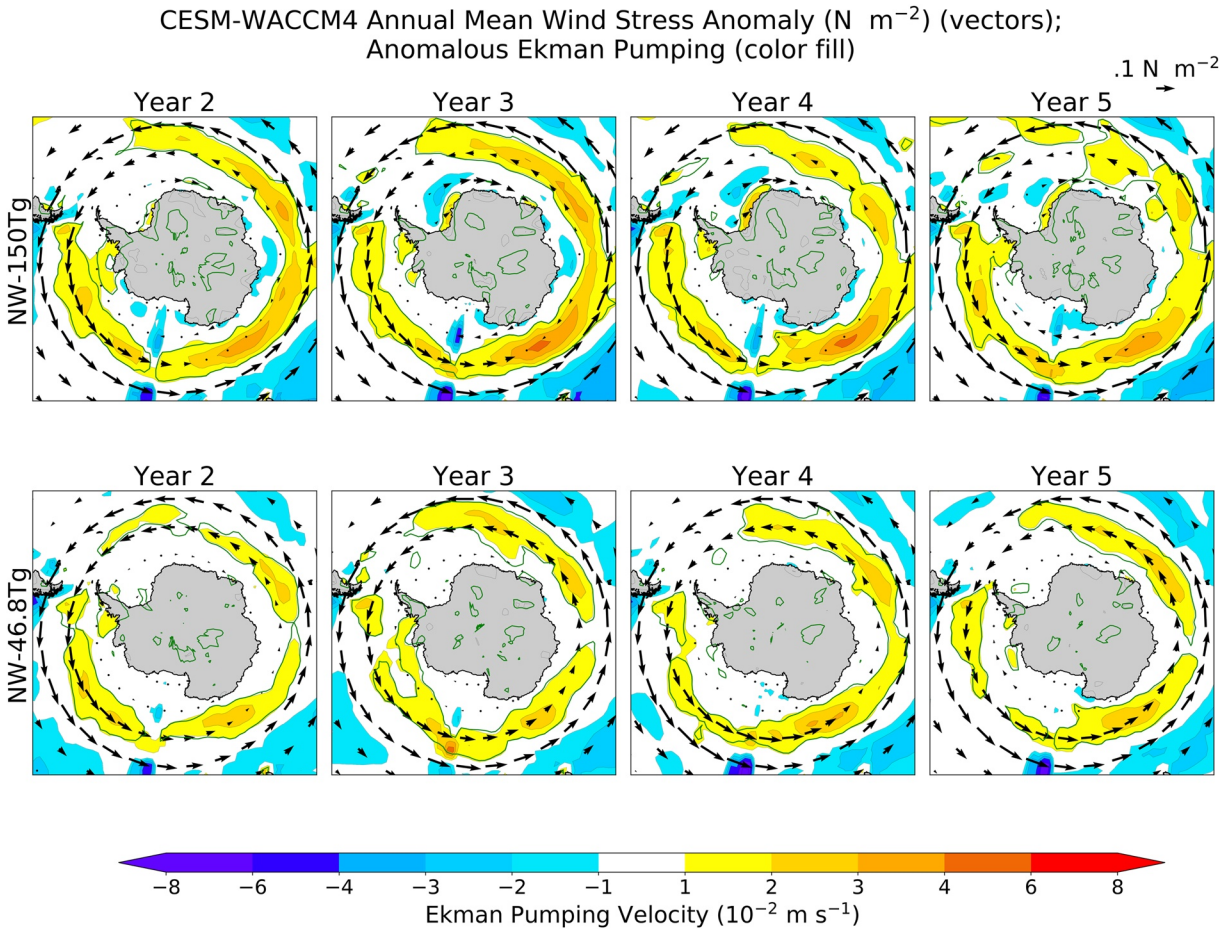

Figure 6. Annual mean surface wind stress anomalies (N m^{-2}, vectors) and anomalous Ekman pumping induced by wind stress curl (10^{-2} m s^{-1}, shading) for NW-150 Tg (top) and NW-46.8 Tg (bottom) between years 2 and 5. The positive wind stress curl anomaly along the coast of the Weddell Sea region drives the upwelling circulation that brings relatively warm subsurface water up and enables sea ice melt. Green contour indicates areas where the anomalies are statistically significant beyond ±2 standard deviations.

salinity (Kurtakoti et al., 2018). The extreme event in 2016 is linked to trends in global warming and the SAM, which help to satisfy the heat content and wind stress curl conditions. Climatic shifts after a large nuclear war can potentially trigger wind shifts as well as high surface salinity due to reduced precipitation globally (Coupe et al., 2019), creating an environment favorable for polynya formation.

After the large nuclear war simulated in NW-150 Tg, an increase in atmospheric pressure over the Weddell Sea weakens the cyclonic atmospheric circulation, contributing to a weakening of both the polar easterlies and the westerlies just to the north. The Weddell Gyre circulation slows in response. The weakened polar easterlies cause a positive zonal wind stress anomaly right along the Antarctic coastline of the Weddell Sea, generating anomalously negative wind stress curl along the coastline (Figure 6), which causes coastal upwelling of relatively warm, salty Weddell Deep Water (Figure 7). As a result, in NW-150 Tg, a polynya forms near the coast, and slowly spreads northward over the course of years 3–5 (Figure 2). In NW-46.8 Tg, changes in atmospheric pressure in the Weddell Sea are smaller, promoting weaker variations in the polar easterlies, and as a result no persistent polynya is simulated. The atmospheric processes responsible for initiating the events that lead to the Weddell Sea polynya in NW-150 Tg are illustrated in Figure 6, which shows how NW-46.8 Tg lacks the wind stress forcing to promote strong coastal upwelling (Figures 6 and 7). The annual mean surface zonal wind stress anomalies are westerly along the Antarctic coastline in the Weddell Sea in NW-150 Tg, which induces Ekman suction along the coastline that is at its strongest between years 3 and 5 post-injection. The relationship between wind stress curl and Ekman velocity is derived from Equation 1:

$$w_E = \nabla \times (\tau / f * \rho) \quad (1)$$

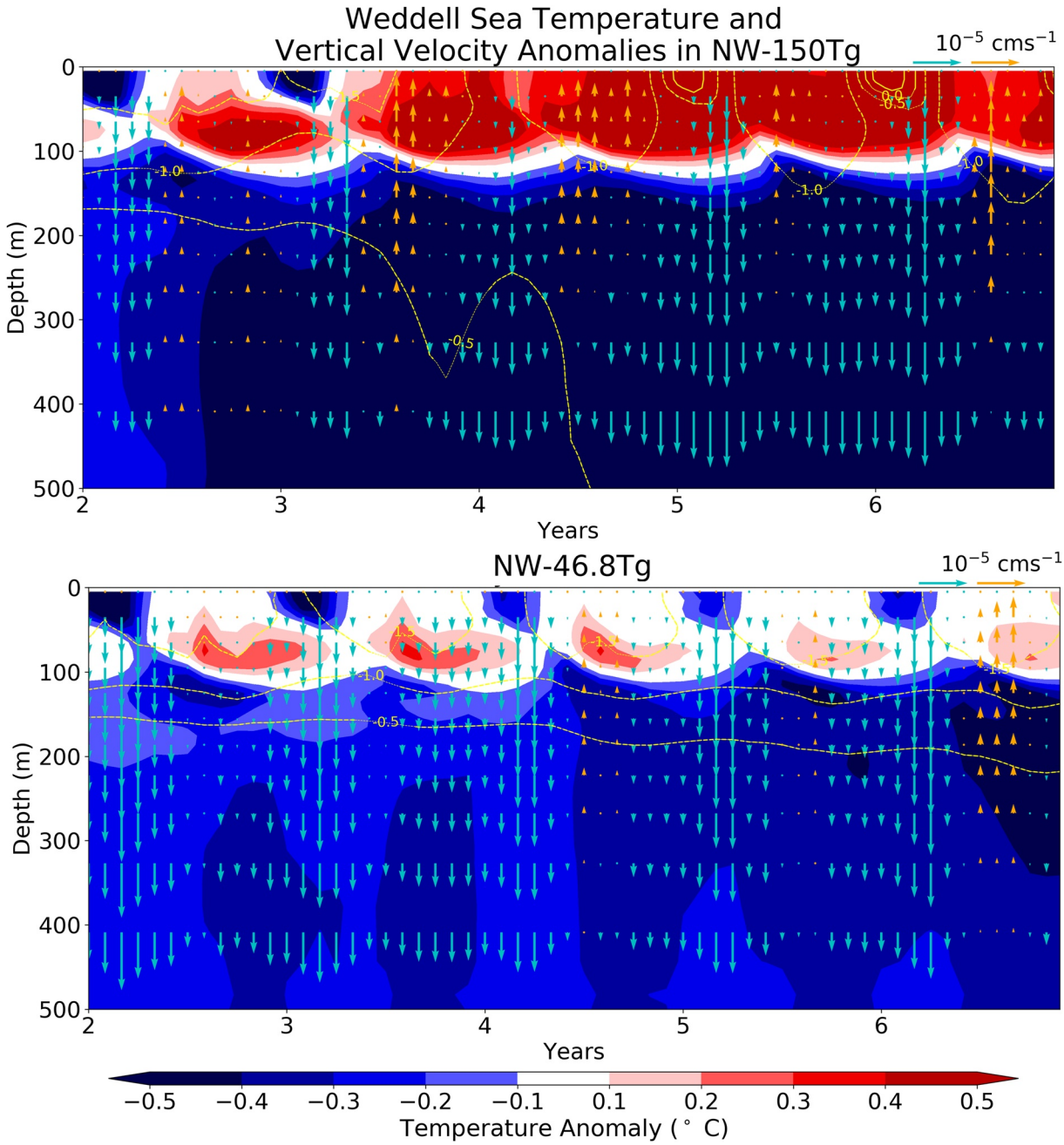

Figure 7. Ocean temperature anomalies (color fill) and vertical velocity anomalies (arrows) in the Weddell Sea for both NW-150 Tg (top) and NW-46.8 Tg (bottom) as a function of depth and time. Orange contours indicate the mean ocean temperatures (°C). Progressive warming in NW-150 Tg is caused by enhanced upwelling in the Weddell Sea.

where w_E is the vertical Ekman velocity, τ is the wind stress, ρ is the density of seawater and f is the Coriolis parameter. In NW-150 Tg, there is positive Ekman velocity (Ekman suctioning) along coastal Antarctica in the southern Weddell Sea, which contributes to the upwelling of warm Weddell Deep Water toward the surface, which is then transported equatorward (Figure 4). Anomalously westerly winds along the coast favor anomalous equatorward Ekman transport of the upwelled water across the gyre (Figure 7), increasing basal melting of the sea ice in the Weddell Sea during the winter and the summer (see Figure S2 in Supporting Information S1 and Movie S1 for visual representation of basal melting). Due to the persistence of the warming signal, sea ice is unable to form again during the winter time, prompting sea ice loss over multiple years. In NW-46.8 Tg, changes in atmospheric pressure in the Weddell Sea cause only small changes to the polar easterlies, resulting in no

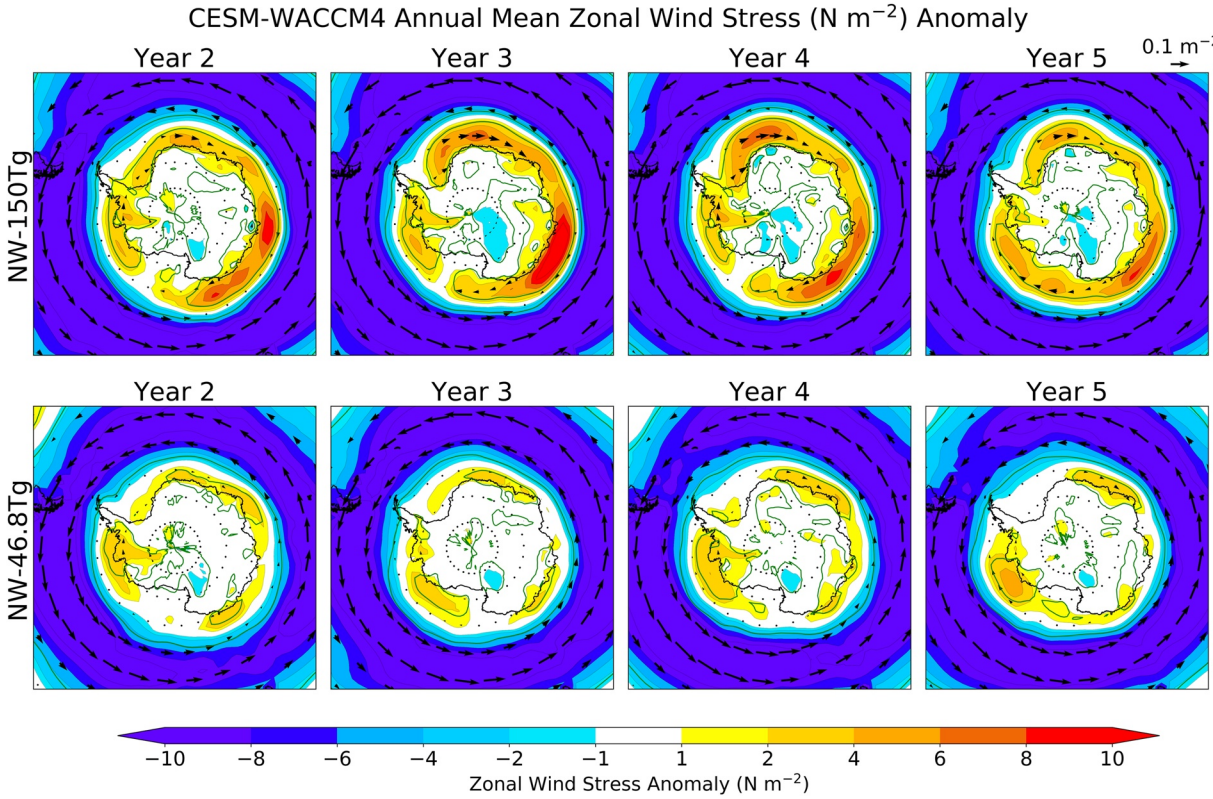

Figure 8. Annual mean zonal wind stress anomaly (color fill and vectors, N m^{-2}) for NW-150 Tg (top) and NW-46.8 Tg (bottom) between years 2 and 5. Green contour indicates areas where the anomalies are statistically significant beyond ±2 standard deviations.

comparably strong Ekman suctioning circulation along the coastline, which explains the absence of a polynya. Because polynyas can lead to a runaway feedback where sea ice is continuously lost (Kurtakoti et al., 2018), the large sea ice disparities in the Weddell Sea between NW-150 Tg and NW-46.8 Tg can be explained by the coastal upwelling circulation only developing in one case.

Even though there is no polynya in NW-46.8 Tg, there is still a warm subsurface temperature anomaly in the Weddell Sea driven by weak coastal upwelling. Figure 7 shows temperature and vertical velocity anomalies averaged over the Weddell Sea for both NW-150 Tg and NW-46.8 Tg through time, illustrating the presence of warmer than average temperatures between 20 and 150 m depth, recurring annually, beginning in the autumn months (March–May). This is in sync with the seasonal cycle of anomalous wind stress. In addition to generating negative wind stress curl, the westerly wind stress anomalies along the Antarctic coastline drive anomalous equatorward Ekman transport and contribute to weak coastal upwelling in the Weddell Sea. In NW-46.8 Tg, weak equatorward Ekman transport along the immediate coastline is the only forcing contributing to coastal upwelling. Thus, the warm anomalies remain just below the surface and are unable to impact sea ice melt in NW-46.8 Tg (Figure 7). Additionally, in NW-46.8 Tg warm anomalies do not persist through winter, in contrast to NW-150 Tg, allowing winter sea-ice growth in the anomalously cold winter water.

3.2.3. Weakened Southern Ocean Westerlies Cause Anomalous Ekman Transport in All Sectors

The final mechanism examined involves the weakening of the westerlies in the Southern Ocean across all longitudes between 50° and 65°S, which explains sea ice loss in all sectors including in the Indian Ocean sector. A strengthened SH stratospheric polar vortex causes a poleward shift in the polar jet and as a result, zonal wind anomalies are positive closer to the coastline of Antarctica but negative further north. The shift in the polar jet occurs in all nuclear war simulations, but the signal is strongest in NW-150 Tg. The surface representation of this wind shift can be seen in Figure 8, which shows zonal mean zonal wind stress anomalies across the Southern Ocean. The shift in the jet is caused by the increase in the pole-to-equator temperature gradient in the lower stratosphere, which happens in both hemispheres.

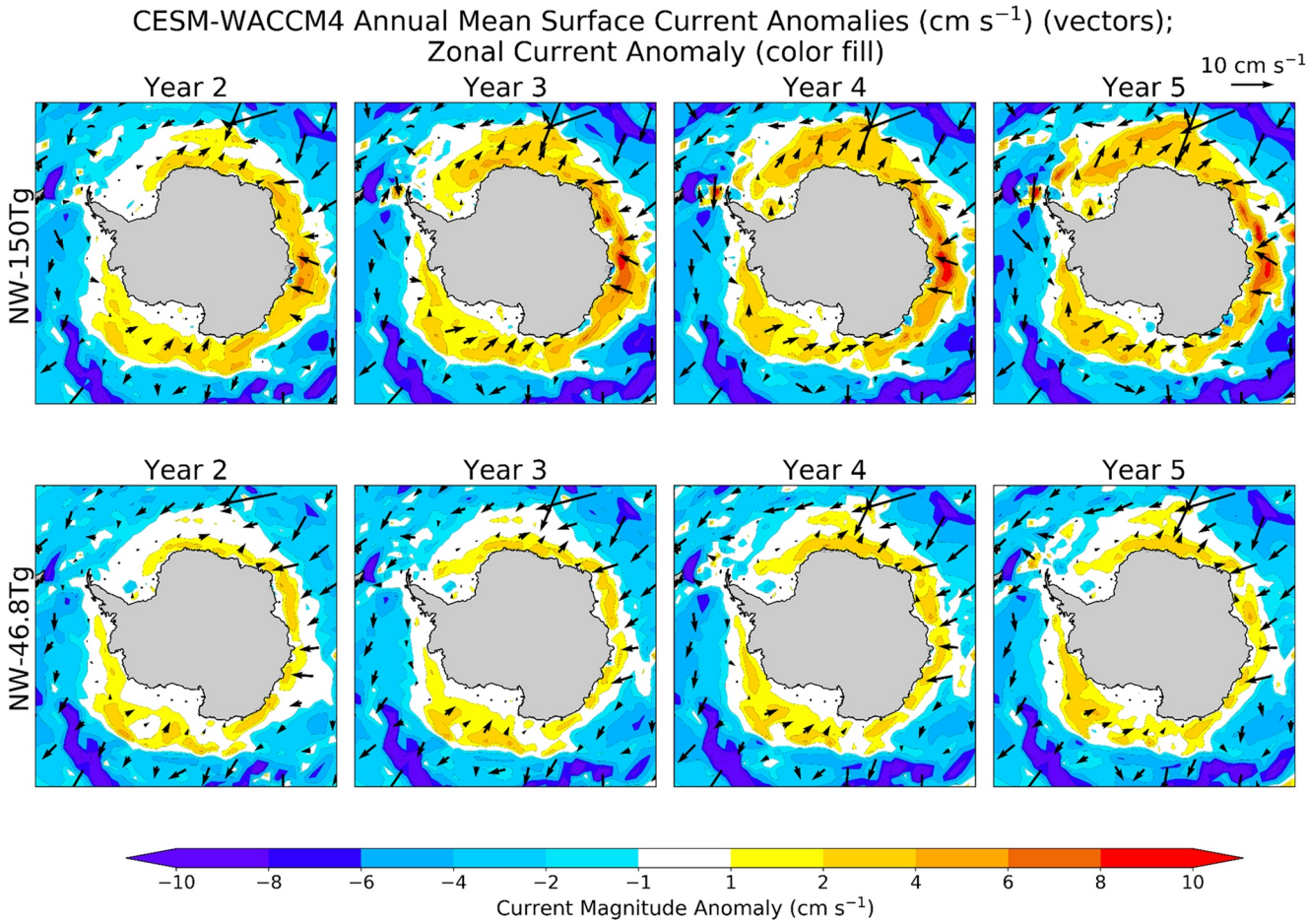

Figure 9. Annual mean surface current anomalies (vectors, cm s^{-1}) and zonal current anomaly (color fill, cm s^{-1}) for NW-150 Tg (top) and NW-46.8 Tg (bottom) between years 2 and 5.

Anomalous poleward advection of relatively warm water occurs along the northern periphery of Antarctic sea ice in all sectors due to the weakening of the westerlies just north of the sea ice. Weakened polar easterlies along the Antarctic coastline and weakened westerlies further north are responsible for both anomalous poleward transport of water from the Southern Ocean and anomalous equatorward transport of water from the coastline of Antarctica. Convergence of water at the surface just offshore is the net result, which causes an accumulation of heat just below the sea ice. An increase in basal melting occurs on the edge of the ice sheet 3 years into NW-150 Tg due to this slow build-up (Movie S1). Basal melting along the equatorward periphery of sea ice is further assisted by the equatorward spreading out of sea ice along the Atlantic and Indian Oceans in NW-150 Tg due to wind stress. The boundary between westerly and easterly wind stress anomalies sits close to the sea ice edge during the winter and spring of years 2 and 3, pushing sea ice equatorward, while the waters of the Southern Ocean experience poleward Ekman drift. Above average sea ice extent along the northern edge of sea ice along the Atlantic and Indian Oceans (see Figure 2) is partially caused by this spreading out of sea ice, which increases its vulnerability to basal melting as warmer waters are advected poleward in years 3 through 5. Easterly wind stress anomalies close to the Antarctic coastline are weaker in NW-46.8 Tg compared to NW-150 Tg, and as a result, sea ice spreading is greater in NW-150 Tg, contributing to a greater loss of SH sea ice volume per area of sea ice compared to NW-46.8 Tg between years 2 and 3.

Additionally, the Antarctic Circumpolar Current (ACC) is weakened (Figure 9), shifting it closer to Antarctic sea ice, increasing the probability of incursions of relatively warm water below the ice (Figure 7). While the ACC in both NW-150 Tg and NW-46.8 Tg are weakened and shifted poleward, the magnitude of the changes in NW-150 Tg are evidently greater and allow for warmer conditions. The weakened Southern Ocean westerlies are thus highly consequential, allowing for heat to accumulate along the coast, which increases basal melting across

all longitudes as a result of poleward Ekman transport of warmer water. This is the primary mechanism affecting sea ice loss in the Indian Ocean sector, where surface currents are anomalously poleward and up to a 40% reduction in sea ice coverage occurs. We note that complex interactions between the ACC and sea ice may not always be captured effectively by the model, but a weakening ACC is qualitatively consistent with the sea ice response.

All sectors of the Southern Ocean are impacted by the weakened and poleward shifted westerlies. In the Indian Ocean, this mechanism accounts for significant losses of sea ice. In the Weddell Sea, it encourages sea ice loss in NW-46.8 Tg, but in NW-150 Tg, negative wind stress curl along the coastline is the instigator for rapid decline. The change in wind stress curl is also connected to the shift in the polar jet, which leads to the vertical advection of heat in the Weddell Sea that acts in concert with the slow horizontal temperature advection in NW-150 Tg.

4. Discussion

We find that a poleward shift in the Southern Ocean westerlies is contributing to warming and loss of sea ice around Antarctica during a nuclear winter. Even with global cooling of nearly 10°C in 2 years following a 150 Tg soot injection, sea ice is sensitive to increased upwelling of relatively warm subsurface waters that occurs with the types of wind shifts that are induced, especially in the Weddell Sea. This work is consistent with previous suggestions that Antarctic sea ice is extremely vulnerable to a sudden global cooling event (McCusker et al., 2015; Verona et al., 2019; Zanchettin et al., 2014), which would only be exacerbated by continued global warming.

In smaller nuclear war simulations with lesser amounts of global cooling, a sudden decline in Antarctic sea ice extent and volume does not occur, indicating a certain threshold of forcing may be required to trigger this response. Because the amount of basal melting depends on the rate of Ekman suctioning and the subsurface temperatures in the Weddell Sea, the threshold where Antarctic sea ice decline occurs is likely sensitive to the initial temperature and sea ice state. In a future scenario where anthropogenic global warming has continued to increase the temperature of the subsurface waters of the Weddell Sea, a global nuclear war could increase the vulnerability of Antarctic sea ice. Outside of a global nuclear war, continuous injection of aerosols into the stratosphere in a potential geoengineering scheme to alleviate anthropogenic global warming may also induce wind shifts that threaten Antarctic sea ice. Future volcanic eruptions in a warmer climate may also lead to reduced sea ice near the Antarctic Peninsula, but only supervolcanic eruptions would exhibit behavior similar to that seen in simulations of nuclear war. Black carbon and organic carbon injections from large-scale wildfires have been investigated as a potential nuclear war analog as well, but these events are unlikely to produce the amount of smoke necessary to provoke the sea ice response after a large-scale nuclear war. The Australian wildfires in December 2019 injected 0.9 Tg of organic and black carbon into the stratosphere, causing local warming in the stratosphere but the annual effective radiative forcing at the surface of -0.32 W m^{-2} produced negligible surface climate impacts (Yu et al., 2021).

While wind stress is the largest contributor to the anomalous Weddell Sea circulation response in our simulations, there are other processes that can influence the density of the surface layer of the Weddell Sea and affect ocean circulation that have not been discussed. For example, the initial response in the first year in NW-150 Tg is a 40% increase in the annual mean volume of Antarctic sea ice. Only in the 27.3 Tg soot simulation does cooling cause a greater expansion in annual mean Antarctic sea ice volume (47%), but it takes 5 years to reach the level achieved in just a year in NW-150 Tg. The rapid expansion of sea ice leaves behind relatively salty water as freshwater is stored as sea ice, increasing the density of the surface of parts of the Southern Ocean (not shown). This brine rejection combined with cooling of the surface ocean from reduced insolation could destabilize the ocean column in proximity to newly formed sea ice, facilitating the same vertical circulation that caused basal melting from shifts in surface wind stress. In this sense, greater cooling and sudden Antarctic sea ice growth beyond a threshold between NW-150 Tg and NW-46.8 Tg could precondition the ocean for a reduction in sea ice. In the two largest cases, Weddell Sea salinity increases by as much as 0.3–0.4 g kg^{-1} and sinking occurs in the Weddell Sea during late summer and autumn, a period typically associated with melting and flux of freshwater into the Southern Ocean. Expanded sea ice increases salt flux into the Southern Ocean and contributes to the anomalous sinking, but positive wind stress curl in NW-150 Tg triggers the upwelling of warm water in the Weddell Sea. Greater brine rejection in NW-150 Tg compared to NW-46.8 Tg is not able to explain the spatial discrepancies in sea ice loss between both cases, particularly in the Weddell Sea. The locations with the greatest sea ice expansion and associated brine rejection occurs outside of the Weddell Sea and along the equatorward periphery of sea ice.

While salinity increases in the top 100 m of the Weddell Sea, most of this occurs after sea ice has already melted and higher salinity water from below is forced upward by positive wind stress curl.

Other factors that may contribute to sea ice loss include the deposition of black carbon onto sea ice, which could theoretically lower the albedo of sea ice and increase absorption of shortwave radiation. Previous work has highlighted the potential for black carbon deposition onto ice sheets after a nuclear war to lower the albedo of snow and ice by up to 30% (Ledley & Thompson, 1986; Warren & Wiscombe, 1985) but Vogelmann et al. (1988) found that by the time there was significant sunlight reaching the ice, the dirty snow had been covered by cleaner snow, so the effect was small. The model used here simulates the deposition of black carbon onto sea ice and the resulting albedo impacts, allowing for this to be quantified. In NW-150 Tg 3 times as much soot is deposited onto sea ice compared to NW-46.8 Tg, so one might reasonably assume the albedo of sea ice could be an important factor in the different response in these two scenarios. However, changes to basal melting are at least one order of magnitude greater than melting from the top of the sea ice (Figure S2 in Supporting Information S1). Ultimately, there is such a significant reduction in solar radiation during a nuclear winter that enhanced melting from darker sea ice or snow is not significant, as in Vogelmann et al. (1988).

Reduced Antarctic sea ice can impact global albedo and the Earth's radiation budget. However, in a nuclear winter, increased sea ice extent in the NH compensates for sea ice loss around Antarctica, nullifying any effects albedo may have on global surface climate. The global ocean circulation is affected by the formation of a polynya in the Weddell Sea, which previously has been found to increase the production of Antarctic Bottom Water (Kurtakoti et al., 2021; Su et al., 2014). Previous work using these same simulations found that nuclear winter related cooling in the North Atlantic would enhance the Atlantic meridional overturning cell (Harrison et al., 2022), and similarly the SH meridional overturning cell is also strengthened.

Reduced Antarctic sea ice extent in a nuclear winter could impact ecosystems that rely on sea ice and exacerbate the ecosystem impacts that are already likely to occur from significantly reduced sunlight and photosynthesis (Coupe et al., 2021; Scherrer et al., 2020). The relationship between Antarctic sea ice extent and ecosystems is complex (Massom & Stammerjohn, 2010). Under normal light conditions, a polynya in the Weddell Sea during Spring could lead to phytoplankton blooms or at least influence the timing of blooms (Massom & Stammerjohn, 2010; von Berg et al., 2020). Open sea ice is more likely to reduce habitat area for organisms that use sea ice to hunt (Steiner et al., 2021). Many of these impacts may be secondary to the dramatic global climate changes and reduced sunlight in a nuclear winter. Ultimately, this work proposes an additional environmental consequence of nuclear war, which may have implications for other events that may inject light absorbing aerosols into the upper atmosphere.

Data Availability Statement

Postprocessed model output is available for the 150 Tg simulation at https://doi.org/10.6084/m9.figshare.7742735.v2 (Coupe, 2019). Postprocessed output for the 5–46.8 Tg simulations can be found at: https://doi.org/10.6084/m9.figshare.14370785.v1 (Coupe, 2021).

Acknowledgments
This work is supported by a grant from the Open Philanthropy Project. This work utilized the RMACC Summit supercomputer, which is supported by the National Science Foundation (awards ACI-1532235 and ACI-1532236), the University of Colorado Boulder, and Colorado State University. The Summit supercomputer is a joint effort of the University of Colorado Boulder and Colorado State University.

References

Bardeen, C. G., Garcia, R. R., Toon, O. B., & Conley, A. J. (2017). On transient climate change at the Cretaceous–Paleogene boundary due to atmospheric soot injections. *Proceedings of the National Academy of Sciences*, *114*(36), E7415–E7424. https://doi.org/10.1073/pnas.1708980114

Cheon, W. G., Lee, S.-K., Gordon, A. L., Liu, Y., Cho, C.-B., & Park, J. J. (2015). Replicating the 1970s' Weddell polynya using a coupled ocean-sea ice model with reanalysis surface flux fields. *Geophysical Research Letters*, *42*(13), 5411–5418. https://doi.org/10.1002/2015GL064364

Coupe, J. (2019). WACCM4 150 Tg US-Russia [Dataset]. figshare. https://doi.org/10.6084/m9.figshare.7742735.v2

Coupe, J. (2021). WACCM4 5 Tg–46.8 Tg India-Pakistan cases [Dataset]. figshare. https://doi.org/10.6084/m9.figshare.14370785.v1

Coupe, J., Bardeen, C. G., Robock, A., & Toon, O. B. (2019). Nuclear winter responses to nuclear war between the United States and Russia in the whole atmosphere community climate model version 4 and the Goddard Institute for Space Studies ModelE. *Journal of Geophysical Research: Atmospheres*, *124*(15), 8522–8543. https://doi.org/10.1029/2019JD030509

Coupe, J., & Robock, A. (2021). The influence of stratospheric soot and sulfate aerosols on the Northern Hemisphere wintertime atmospheric circulation. *Journal of Geophysical Research: Atmospheres*, *126*(11), e2020JD034513. https://doi.org/10.1029/2020JD034513

Coupe, J., Stevenson, S., Lovenduski, N. S., Rohr, T., Harrison, C. S., Robock, A., et al. (2021). Nuclear Niño response observed in simulations of nuclear war scenarios. *Communications Earth & Environment*, *2*(1), 1–11. https://doi.org/10.1038/s43247-020-00088-1

CPC - Teleconnections. (2021). Antarctic Oscillation. Retrieved from https://www.cpc.ncep.noaa.gov/products/precip/CWlink/daily_ao_index/aao/aao.shtml

Danabasoglu, G., Bates, S. C., Briegleb, B. P., Jayne, S. R., Jochum, M., Large, W. G., et al. (2012). The CCSM4 ocean component. *Journal of Climate*, *25*(5), 1361–1389. https://doi.org/10.1175/JCLI-D-11-00091.1

Ding, Q., Steig, E. J., Battisti, D. S., & Wallace, J. M. (2012). Influence of the tropics on the southern annular mode. *Journal of Climate*, *25*(18), 6330–6348. https://doi.org/10.1175/JCLI-D-11-00523.1

Dinniman, M. S., Klinck, J. M., & Hofmann, E. E. (2012). Sensitivity of circumpolar deep water transport and ice shelf basal melt along the West Antarctic Peninsula to changes in the winds. *Journal of Climate*, *25*(14), 4799–4816. https://doi.org/10.1175/JCLI-D-11-00307.1

Fyfe, J. C., Saenko, O. A., Zickfeld, K., Eby, M., & Weaver, A. J. (2007). The role of poleward-intensifying winds on Southern Ocean warming. *Journal of Climate*, *20*(21), 5391–5400. https://doi.org/10.1175/2007JCLI1764.1

Harrison, C. S., Rohr, T., DuVivier, A., Maroon, E. A., Bachman, S., Bardeen, C. G., et al. (2022). A new ocean state after nuclear war. *AGU Advances*, *3*(4), e2021AV000610. https://doi.org/10.1029/2021AV000610

Hirabara, M., Tsujino, H., Nakano, H., & Yamanaka, G. (2012). Formation mechanism of the Weddell Sea Polynya and the impact on the global abyssal ocean. *Journal of Oceanography*, *68*(5), 771–796. https://doi.org/10.1007/s10872-012-0139-3

Hunke, E. C., & Lipscomb, W. H. (2008). *CICE: The Los Alamos sea ice model documentation and software version 4.0* (p. 76). Los Alamos National Laboratory.

Kay, E. J., Deser, C., Phillips, A., Mai, A. W., Hannay, C., Strand, G., et al. (2015). The Community Earth System Model (CESM) large ensemble project: A community resource for studying climate change in the presence of internal climate variability. *Bulletin of the American Meteorological Society*, *96*(8), 1333–1349. https://doi.org/10.1175/BAMS-D-13-00255.1

Kurtakoti, P., Veneziani, M., Stössel, A., & Weijer, W. (2018). Preconditioning and formation of Maud Rise polynyas in a high-resolution Earth system model. *Journal of Climate*, *31*(23), 9659–9678. https://doi.org/10.1175/JCLI-D-18-0392.1

Kurtakoti, P., Veneziani, M., Stössel, A., Weijer, W., & Maltrud, M. (2021). On the generation of Weddell Sea polynyas in a high-resolution Earth system model. *Journal of Climate*, *34*(7), 2491–2510. https://doi.org/10.1175/JCLI-D-20-0229.1

Lachlan-Cope, T., & Connolley, W. (2006). Teleconnections between the tropical Pacific and the Amundsen-Bellinghausens Sea: Role of the El Niño/Southern Oscillation. *Journal of Geophysical Research*, *111*(D23), D23101. https://doi.org/10.1029/2005JD006386

Ledley, T. S., & Thompson, S. L. (1986). Potential effect of nuclear war smokefall on sea ice. *Climatic Change*, *8*(2), 155–171. https://doi.org/10.1007/BF00139752

Marsh, D. R., Mills, M. J., Kinnison, D. E., Lamarque, J.-F., Calvo, N., & Polvani, L. M. (2013). Climate change from 1850 to 2005 simulated in CESM1(WACCM). *Journal of Climate*, *26*(19), 7372–7391. https://doi.org/10.1175/JCLI-D-12-00558.1

Massom, R. A., & Stammerjohn, S. E. (2010). Antarctic sea ice change and variability – Physical and ecological implications. *Polar Science*, *4*(2), 149–186. https://doi.org/10.1016/j.polar.2010.05.001

Mayewski, P. A., Meredith, M. P., Summerhayes, C. P., Turner, J., Worby, A., Barrett, P. J., et al. (2009). State of the Antarctic and Southern Ocean climate system. *Reviews of Geophysics*, *47*(1), RG1003. https://doi.org/10.1029/2007RG000231

McCusker, K. E., Battisti, D. S., & Bitz, C. M. (2015). Inability of stratospheric sulfate aerosol injections to preserve the West Antarctic Ice Sheet. *Geophysical Research Letters*, *42*(12), 4989–4997. https://doi.org/10.1002/2015GL064314

Meehl, G. A., Arblaster, J. M., Chung, C. T. Y., Holland, M. M., DuVivier, A., Thompson, L., et al. (2019). Sustained ocean changes contributed to sudden Antarctic sea ice retreat in late 2016. *Nature Communications*, *10*(1), 14. https://doi.org/10.1038/s41467-018-07865-9

Paolo, F. S., Padman, L., Fricker, H. A., Adusumilli, S., Howard, S., & Siegfried, M. R. (2018). Response of Pacific-sector Antarctic ice shelves to the El Niño/Southern Oscillation. *Nature Geoscience*, *11*(2), 121–126. https://doi.org/10.1038/s41561-017-0033-0

Raphael, M. N., Marshall, G. J., Turner, J., Fogt, R. L., Schneider, D., Dixon, D. A., et al. (2016). The Amundsen sea low: Variability, change, and impact on Antarctic climate. *Bulletin of the American Meteorological Society*, *97*(1), 111–121. https://doi.org/10.1175/BAMS-D-14-00018.1

Reese, R., Gudmundsson, G. H., Levermann, A., & Winkelmann, R. (2018). The far reach of ice-shelf thinning in Antarctica. *Nature Climate Change*, *8*(1), 53–57. https://doi.org/10.1038/s41558-017-0020-x

Robock, A. (2000). Volcanic eruptions and climate. *Reviews of Geophysics*, *38*(2), 191–219. https://doi.org/10.1029/1998RG000054

Robock, A., Oman, L., & Stenchikov, G. L. (2007). Nuclear winter revisited with a modern climate model and current nuclear arsenals: Still catastrophic consequences. *Journal of Geophysical Research*, *112*(D13), D13107. https://doi.org/10.1029/2006JD008235

Scherrer, K. J. N., Harrison, C. S., Heneghan, R. F., Galbraith, E., Bardeen, C. G., Coupe, J., et al. (2020). Marine wild-capture fisheries after nuclear war. *Proceedings of the National Academy of Sciences*, *117*(47), 29748–29758. https://doi.org/10.1073/pnas.2008256117

Singh, H. K. A., Landrum, L., Holland, M. M., Bailey, D. A., & DuVivier, A. K. (2021). An overview of Antarctic sea ice in the Community Earth System Model version 2, Part I: Analysis of the seasonal cycle in the context of sea ice thermodynamics and coupled atmosphere-ocean-ice processes. *Journal of Advances in Modeling Earth Systems*, *13*(3), e2020MS002143. https://doi.org/10.1029/2020MS002143

Smith, K. L., Polvani, L. M., & Marsh, D. R. (2012). Mitigation of 21st century Antarctic sea ice loss by stratospheric ozone recovery. *Geophysical Research Letters*, *39*(20), L20701. https://doi.org/10.1029/2012GL053325

Spence, P., Griffies, S. M., England, M. H., Hogg, A. M., Saenko, O. A., & Jourdain, N. C. (2014). Rapid subsurface warming and circulation changes of Antarctic coastal waters by poleward shifting winds. *Geophysical Research Letters*, *41*(13), 4601–4610. https://doi.org/10.1002/2014GL060613

Stammerjohn, S. E., Martinson, D. G., Smith, R. C., Yuan, X., & Rind, D. (2008). Trends in Antarctic annual sea ice retreat and advance and their relation to El Niño–Southern Oscillation and Southern Annular Mode variability. *Journal of Geophysical Research*, *113*(C3), C03S90. https://doi.org/10.1029/2007JC004269

Steiner, N. S., Bowman, J., Campbell, K., Chierici, M., Eronen-Rasimus, E., Falardeau, M., et al. (2021). Climate change impacts on sea-ice ecosystems and associated ecosystem services. *Elementa: Science of the Anthropocene*, *9*(1), 00007. https://doi.org/10.1525/elementa.2021.00007

Su, Z., Stewart, A. L., & Thompson, A. F. (2014). An idealized model of Weddell Gyre export variability. *Journal of Physical Oceanography*, *44*(6), 1671–1688. https://doi.org/10.1175/JPO-D-13-0263.1

Toon, O. B., Bardeen, C. G., Robock, A., Xia, L., Kristensen, H., McKinzie, M., et al. (2019). Rapidly expanding nuclear arsenals in Pakistan and India portend regional and global catastrophe. *Science Advances*, *5*(10), eaay5478. https://doi.org/10.1126/sciadv.aay5478

Turner, J., Phillips, T., Marshall, G. J., Hosking, J. S., Pope, J. O., Bracegirdle, T. J., & Deb, P. (2017). Unprecedented springtime retreat of Antarctic sea ice in 2016. *Geophysical Research Letters*, *44*(13), 6868–6875. https://doi.org/10.1002/2017GL073656

Verona, L. S., Wainer, I., & Stevenson, S. (2019). Volcanically triggered ocean warming near the Antarctic Peninsula. *Scientific Reports*, *9*(1), 9462. https://doi.org/10.1038/s41598-019-45190-3

Vogelmann, A., Robock, A., & Ellingson, R. (1988). Effects of dirty snow in nuclear winter simulations. *Journal of Geophysical Research*, *93*(D5), 5319–5332. https://doi.org/10.1029/JD093ID05P05319

von Berg, L., Prend, C. J., Campbell, E. C., Mazloff, M. R., Talley, L. D., & Gille, S. T. (2020). Weddell Sea phytoplankton blooms modulated by sea ice variability and polynya formation. *Geophysical Research Letters*, *47*(11), e2020GL087954. https://doi.org/10.1029/2020GL087954

Warren, S. G., & Wiscombe, W. J. (1985). Dirty snow after nuclear war. *Nature*, *313*(6002), 467–470. https://doi.org/10.1038/313467a0

Xia, L., Robock, A., Scherrer, K., Harrison, C. S., Bodirsky, B. L., Weindl, I., et al. (2022). Global food insecurity and famine from reduced crop, marine fishery and livestock production due to climate disruption from nuclear war soot injection. *Nature Food*, *3*(8), 586–596. https://doi.org/10.1038/s43016-022-00573-0

Yu, P., Davis, S. M., Toon, O. B., Portmann, R. W., Bardeen, C. G., Barnes, J. E., et al. (2021). Persistent stratospheric warming due to 2019–2020 Australian wildfire smoke. *Geophysical Research Letters*, *48*(7), e2021GL092609. https://doi.org/10.1029/2021GL092609

Zanchettin, D., Bothe, O., Timmreck, C., Bader, J., Beitsch, A., Graf, H.-F., et al. (2014). Inter-hemispheric asymmetry in the sea-ice response to volcanic forcing simulated by MPI-ESM (COSMOS-Mill). *Earth System Dynamics*, *5*(1), 223–242. https://doi.org/10.5194/esd-5-223-2014